Kinetics of free radical styrene polymerization with the symmetrical bifunctional initiator 2,5-dimethyl-2,5-bis(2-ethyl hexanoyl peroxy)hexane

Won Jung Yoon and Kyu Yong Choi*
Department of Chemical Engineering, University of Maryland, College Park, MD 20742, USA
(Received 1 August 1991; revised 1 January 1992; accepted 11 February 1992)

The kinetics of bulk free radical polymerization of sytrene is studied with the symmetrical bifunctional initiator 2,5-dimethyl-2,5-bis(2-ethyl hexanoyl peroxy)hexane. The initiator, monomers and live polymers undergo complex initiation, propagation, chain transfer and chain termination reactions due to the presence of two labile peroxide groups of equal thermal stabilities in the initiator. The effects of reaction temperature and initiator concentration on the polymerization rate and polymer molecular weight properties have been investigated. It is shown that the composition of a polymerizing mixture is influenced by the initiator concentration and reaction temperature. The apparent initiator efficiency factor was found to decrease as the initiator concentration increased. A detailed kinetic model is also presented and used to analyse the fate of peroxide groups during the course of polymerization.

(Keywords: styrene polymerization; symmetrical bifunctional initiator; bulk polymerization; initiator efficiency)

INTRODUCTION

Bifunctional initiators containing two labile groups (e.g. peroxides or azo groups) are frequently used in the polymer industry for the synthesis of vinyl polymers and resin curing. In general, there are two types of bifunctional initiators: (i) symmetrical bifunctional initiators containing two identical labile groups of equal thermal stability; and (ii) unsymmetrical bifunctional initiators containing two labile groups of unequal thermal stabilities. One of the potential advantages of using bifunctional initiators is that high polymer molecular weight and high polymerization rate can be obtained simultaneously by controlling the initiator decomposition rate through optimal reactor temperature programming. The other application of the bifunctional or multifunctional initiators also lies in the possibility of making block copolymers by a two-stage radical process. For the most efficient utilization of bifunctional initiators, it is essential to have a quantitative kinetic model and have it validated experimentally.

For free radical styrene polymerization with monofunctional initiators, the reaction kinetics are reasonably well understood in both low and high monomer conversion regimes. However, the presence of an additional labile group in bifunctional initiators makes the polymerization kinetics very complicated. This is because labile groups such as peroxides become redistributed repeatedly in the growing and inactive polymers and they are engaged in further initiation, propagation, chain transfer and termination reactions during the course of polymerization. We have reported the kinetic models for free radical styrene polymerization with symmetrical and unsymmetrical bifunctional initiators[1–4]. Recently, Villalobos *et al.*[5] investigated the kinetics of styrene polymerization with several commercially available bifunctional initiators.

In this paper, the kinetics of bulk styrene polymerization with a commercial symmetrical bifunctional initiator is investigated through detailed kinetic modelling and laboratory experimentation. The kinetic model we proposed earlier is modified to include the effects of primary diradical formation, thermal initiation and volume change during the polymerization. The effects of reaction temperature and initiator concentration on the polymerization rate and molecular weight are investigated. In particular, the fate of undecomposed peroxide groups in the initiator and the polymers is analysed via model simulations.

REACTION KINETICS

The symmetrical bifunctional initiator considered in this study is a diperoxyester of the following form:

$$R_1-\overset{\overset{O}{\|}}{C}-OO-R_2-OO-\overset{\overset{O}{\|}}{C}-R_1 \qquad (1)$$

where R_1 and R_2 represent hydrocarbon ligands. The specific bifunctional initiator of the above structure used in our experimental study is 2,5-dimethyl-2,5-bis(2-ethyl hexanoyl peroxy)hexane (Lupersol 256, ATOCHEM)

*To whom correspondence should be addressed
0032-3861/92/214582-10

which is commercially available:

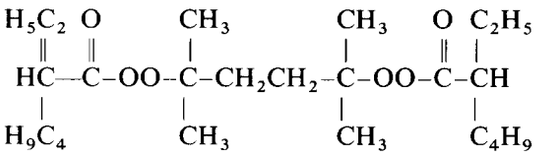

I (2)

This initiator is a liquid at room temperature and the peroxide half-life at 100°C is 21 min. Upon heating, the initiator (I) decomposes to generate two different primary radical species:

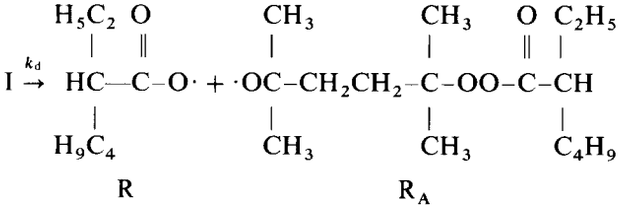

(3)

The route that the peroxyester decomposition proceeds depends on the stability of each radical species produced by the above homolytic scission reaction. The radical species R_A containing an undecomposed peroxide may decompose further to yield R and a diradical species (R′):

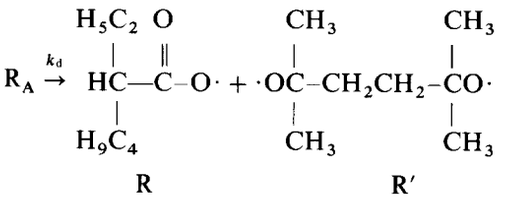

(4)

The primary radical species R and R_A may also undergo decarboxylation and β-scission reaction, respectively; however, there will be no net change in the radical concentration as a result of such reactions. Since the peroxide groups are separated by a fairly long hydrocarbon bridge for an inductive effect being negligible, the decomposition rate constant is assumed to be unaffected by whether or not the neighbouring peroxide group has decomposed. It is also assumed that the peroxide groups in the polymer chain ends have the same decomposition rate constant as the peroxide groups in the original bifunctional initiator. It is assumed that branching reactions due to hydrogen abstraction by chain transfer to polymer do not occur in styrene polymerization. The polymer chain initiated by R_A radicals will have an undecomposed peroxide which may decompose to generate new radical species during the course of polymerization, making the overall initiation process quite complex.

For the modelling of the polymerization kinetics, a molecular species modelling technique is used. Here, the polymer molecules are identified by the type of their end units as shown in *Table 1*. The subscript n indicates the number of repeating units in the polymer chain. Polymer species Q_n, Z_n and T_n contain one or two undecomposed peroxides which are subject to further decomposition reactions. Then, we can postulate that the polymerization will proceed as shown in *Table 2*. Note that both the primary initiator and T_n species have dual functionality because they contain two undecomposed peroxide groups. We assume that the thermal stability of the peroxides in polymer chains is independent of the polymer chain length. The termination by primary

Table 1 Polymeric species in free radical polymerization initiated by a symmetrical bifunctional initiator

P_n	●————]
Q_n	●————CO–OOR$_1$
S_n	●————●
T_n	R$_1$OO–OC————CO–OOR$_1$
Z_n	[————CO–OOR$_1$
M'_n	[————]

●, Free radical; ——], polymer chain with inactive chain end

Table 2 Kinetic scheme with a bifunctional initiator

Peroxide decomposition reactions

$$I \xrightarrow{2k_d} R + R_A$$

$$R_A \xrightarrow{k_d} R + R'$$

$$Q_n \xrightarrow{k_d} S_n + R \qquad (n \geq 1)$$

$$T_n \xrightarrow{2k_d} Q_n + R \qquad (n \geq 2)$$

$$Z_n \xrightarrow{k_d} P_n + R \qquad (n \geq 1)$$

Initiation reactions

$$R + M \xrightarrow{k_i} P_1$$

$$R_A + M \xrightarrow{k_i} Q_1$$

$$R' + M \xrightarrow{2k_i} S_1$$

$$3M \xrightarrow{k_m} 2P_1$$

Propagation reactions ($n \geq 1$)

$$P_n + M \xrightarrow{k_p} P_{n+1}$$

$$Q_n + M \xrightarrow{k_p} Q_{n+1}$$

$$S_n + M \xrightarrow{2k_p} S_{n+1}$$

Chain transfer reactions to monomer ($n \geq 1$)

$$P_n + M \xrightarrow{k_{fm}} M'_n + P_1$$

$$Q_n + M \xrightarrow{k_{fm}} Z_n + P_1$$

$$S_n + M \xrightarrow{2k_{fm}} P_n + P_1$$

Termination reactions ($n, m \geq 1$)

$$P_n + P_m \xrightarrow{k_t} M'_{n+m}$$

$$P_n + Q_m \xrightarrow{k_t} Z_{n+m}$$

$$P_n + S_m \xrightarrow{2k_t} P_{n+m}$$

$$Q_n + Q_m \xrightarrow{k_t} T_{n+m}$$

$$Q_n + S_m \xrightarrow{2k_t} Q_{n+m}$$

$$S_n + S_m \xrightarrow{4k_t} S_{n+m}$$

radicals is assumed negligible in the above scheme. It is also assumed that the combination termination rate constants for the macroradical species are identical. In order to account for the diffusion controlled termination or the gel effect, an empirical correlation reported by Friis and Hamielec[6] is used.

With the kinetic scheme shown in *Table 2*, rate expressions can be developed for each species in the polymerization mixture as follows.

For initiator and primary radicals:

$$\frac{1}{V}\frac{d(IV)}{dt} = -2k_d I \tag{5}$$

$$\frac{1}{V}\frac{d(RV)}{dt} = 2f_i k_d I - k_i RM + f_i k_d R_A + f_i k_d (Q + 2T + Z) \tag{6}$$

$$\frac{1}{V}\frac{d(R_A V)}{dt} = 2f_i k_d I - k_i R_A M - k_d R_A \tag{7}$$

$$\frac{1}{V}\frac{d(R'V)}{dt} = f_i k_d R_A - 2k_i R'M \tag{8}$$

For growing polymers:

$$\frac{1}{V}\frac{d(P_1 V)}{dt} = 2k_m M^3 + k_i RM + k_{d_2} Z_1 + k_{fm} M(P - P_1 + Q + 2S + 2S_1) - k_p M P_1 - k_t P_1 (P + Q + 2S) \tag{9a}$$

$$\frac{1}{V}\frac{d(P_n V)}{dt} = k_d Z_n + k_{fm} M(2S_n - P_n) + k_p M(P_{n-1} - P_n) - k_t P_n (P + Q + 2S) + 2k_t \sum_{m=1}^{n-1} P_{n-m} S_m \quad (n \geqslant 2) \tag{9b}$$

$$\frac{1}{V}\frac{d(Q_1 V)}{dt} = k_i R_A M - k_d Q_1 - k_{fm} M Q_1 - k_p M Q_1 - k_t Q_1 (P + Q + 2S) \tag{10a}$$

$$\frac{1}{V}\frac{d(Q_n V)}{dt} = k_d (2T_n - Q_n) - k_{fm} M Q_n + k_p M(Q_{n-1} - Q_n) - k_t Q_n (P + Q + 2S) + 2k_t \sum_{m=1}^{n-1} Q_{n-m} S_m \quad (n \geqslant 2) \tag{10b}$$

$$\frac{1}{V}\frac{d(S_1 V)}{dt} = 2k_i R'M + k_d Q_1 - 2k_{fm} M S_1 - 2k_p M S_1 - 2k_t S_1 (P + Q + 2S) \tag{11a}$$

$$\frac{1}{V}\frac{d(S_n V)}{dt} = k_d Q_n - 2k_{fm} M S_n + 2k_p M(S_{n-1} - S_n) - 2k_t S_n (P + Q + 2S) + 2k_t \sum_{m=1}^{n-1} S_{n-m} S_m \quad (n \geqslant 2) \tag{11b}$$

For temporarily inactive polymers:

$$\frac{1}{V}\frac{d(T_n V)}{dt} = -2k_d T_n + \frac{k_t}{2} \sum_{m=1}^{n-1} Q_{n-m} Q_m \quad (n \geqslant 2) \tag{12}$$

$$\frac{1}{V}\frac{d(Z_1 V)}{dt} = -k_d Z_1 + k_{fm} M Q_1 \tag{13a}$$

$$\frac{1}{V}\frac{d(Z_n V)}{dt} = -k_d Z_n + k_{fm} M Q_n + k_t \sum_{m=1}^{n-1} P_{n-m} Q_m \quad (n \geqslant 2) \tag{13b}$$

For monomers and dead polymers:

$$\frac{1}{V}\frac{d(MV)}{dt} = -k_p M(P + Q + 2S) \tag{14}$$

$$\frac{1}{V}\frac{d(M_n' V)}{dt} = k_{fm} M P_n + \frac{k_t}{2} \sum_{m=1}^{n-1} P_{n-m} P_m \quad (n \geqslant 2) \tag{15}$$

In the above equations, V is the volume of the reaction mixture and f_i is the initiator efficiency factor which represents the fraction of primary radicals being involved in chain initiation. It is assumed that monomer consumption through initiation reactions and chain transfer to monomer is negligible and that the initiator efficiency is constant during the polymerization. P, Q, S, T and Z are the total concentrations of the corresponding polymeric species, i.e.

$$P = \sum_{n=1}^{\infty} P_n \qquad Q = \sum_{n=1}^{\infty} Q_n \qquad S = \sum_{n=1}^{\infty} S_n$$
$$T = \sum_{n=2}^{\infty} T_n \qquad Z = \sum_{n=1}^{\infty} Z_n \tag{16}$$

The number average molecular weight (M_n) and the weight average molecular weight (M_w) are calculated using the molecular weight moments. The moment equations are summarized in the Appendix. The computational method using the molecular weight moment is well described in reference 7. The numerical values of kinetic parameters and physical constants used in our model simulations are listed in *Table 3*. The following equation is used to account for the volume change during the polymerization:

$$\frac{1}{V}\frac{dV}{dt} = -\frac{\varepsilon}{(M_0 + \varepsilon M)}\frac{dM}{dt} \tag{17}$$

where M_0 is the initial monomer concentration, V the

Table 3 Kinetic parameters and physical constants

	Ref.
k_d (min^{-1}) = $1.251 \times 10^{17} \exp(-31\,700/RT)$	8
k_m (l^2 mol^{-2} min^{-1}) = $1.314 \times 10^7 \exp(-27\,440/RT)$	9
k_p (l mol^{-1} min^{-1}) = $6.306 \times 10^8 \exp(-7060/RT)$	10
k_{t0} (l mol^{-1} min^{-1}) = $7.530 \times 10^{10} \exp(-1680/RT)$	10
k_i (l mol^{-1} min^{-1}) = $6.306 \times 10^8 \exp(-7060/RT)$	10
$k_{fm,0}$ (l mol^{-1} min^{-1}) = $2.319 \times 10^8 \exp(-10\,790/RT)$	
M_0 (mol l^{-1}) = 8.728	
$\varepsilon = -0.147$	11
$g_t \equiv \frac{k_t}{k_{t0}} = \exp[-2(Bx + Cx^2 + Dx^3)]$	3, 6
$B = 2.5882 - 3.4852 \times 10^{-3} T$	
$C = 4.3108 - 1.2635 \times 10^{-2} T$	
$D = -4.6488 + 1.9026 \times 10^{-2} T$	

volume of the polymerizing mixture, and ε the volume contraction factor defined by:

$$\varepsilon = \frac{V_{x=1} - V_{x=0}}{V_{x=0}} \tag{18}$$

where x is the fractional momomer conversion.

EXPERIMENTAL

Polymerization experiments were carried out using Pyrex ampoules (o.d. 5 mm). Styrene (Aldrich) was passed through an Amberlyst-27 column (Rohm and Hass) to remove inhibitors. The bifunctional initiator (Lupersol 256), containing 90% peroxide in decane, was used as supplied. Each ampoule containing monomer and initiator was purged with nitrogen and degassed by many successive freeze–thaw cycles in acetone and dry ice mixture until the bubbles could not be seen. An oil bath was used to keep the ampoules at a desired temperature. Once the heating bath reached the desired reaction temperature, all the ampoules were dipped into the bath. After the reaction, the polymer samples were dissolved in toluene and precipitated by adding excess methanol. This procedure was repeated several times to ensure that unreacted monomer was completely removed from the polymer. The samples were dried *in vacuo*, and the monomer conversion was measured by the gravimetric method. The experiments were duplicated and the reproducibilities of the experimental data were excellent. In order to confirm the isothermal reaction conditions, several test experiments were conducted by inserting a thermocouple into the ampoule and monitoring the reaction temperature. For the reaction temperatures employed in this work, the maximum temperature difference between the oil bath and the reaction mixture in the ampoule was 0.8°C. The polymer molecular weight and molecular weight distribution were determined by g.p.c. with four Ultrastyragel columns (Waters; 10^4, 10^3, 500 Å, and linear) and tetrahydrofuran (THF) as a solvent. These columns were calibrated using several commercially available polystyrene samples of known molecular weight.

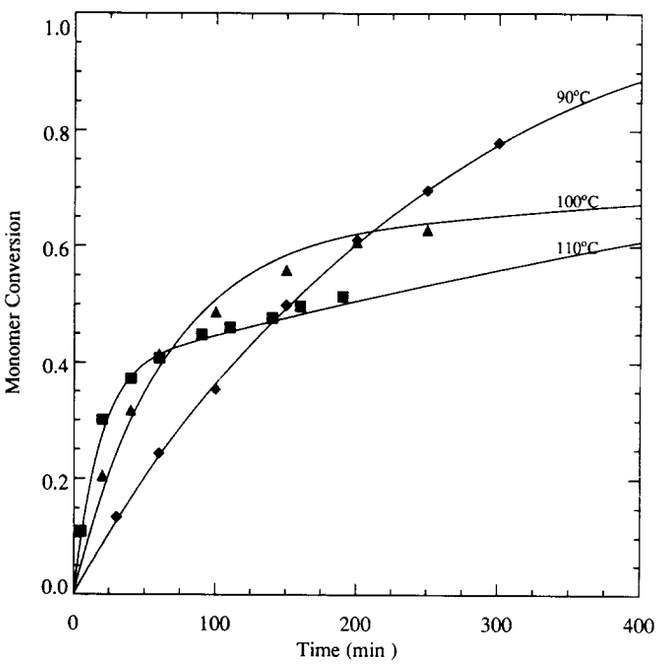

Figure 1 Effect of polymerization temperature on monomer conversion ($I_0 = 0.005$ mol l^{-1}; - —, model prediction)

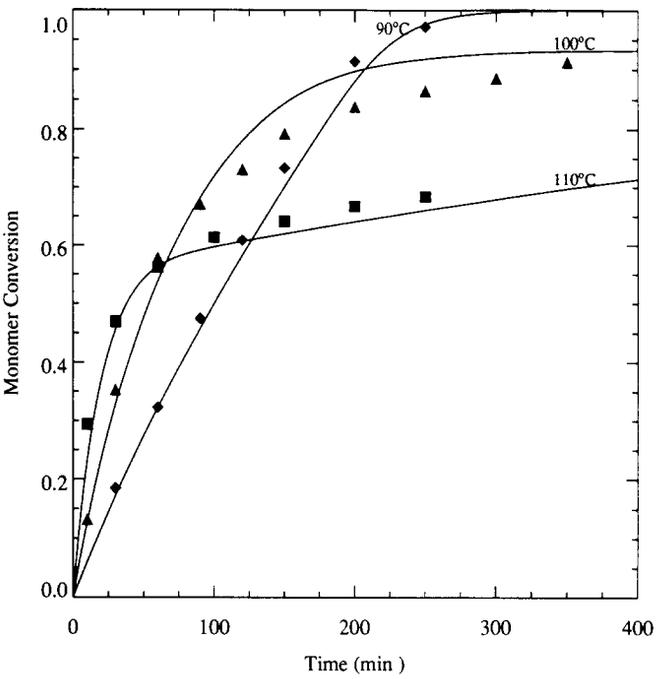

Figure 2 Effect of polymerization temperature on monomer conversion ($I_0 = 0.01$ mol l^{-1}; ——, model prediction)

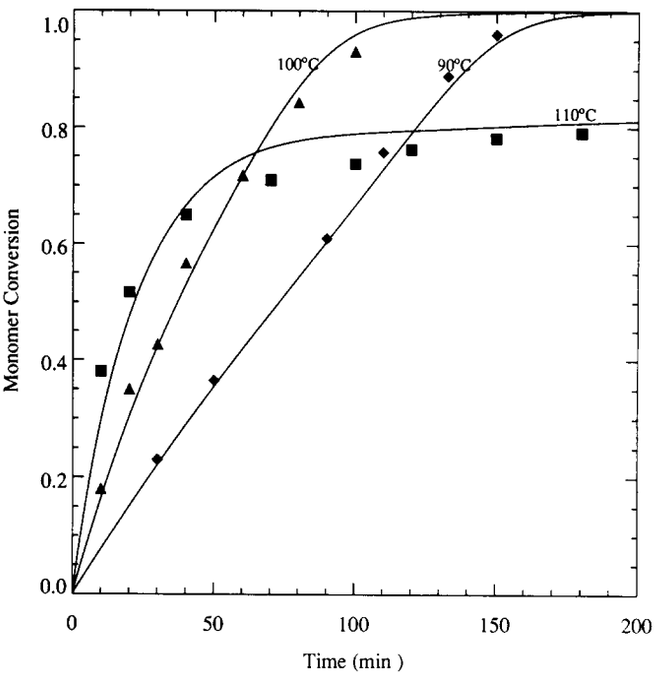

Figure 3 Effect of polymerization temperature on monomer conversion ($I_0 = 0.02$ mol l^{-1}; ——, model prediction)

RESULTS AND DISCUSSION

The bifunctional initiator used (Lupersol 256) is known to be most effective at reaction temperatures around 90–100°C. Thus, the effect of reaction temperature on the polymerization kinetics was first investigated at three different temperatures (90, 100 and 110°C). *Figures 1–3* show the monomer conversion profiles for the initiator concentration (I_0) of 0.005, 0.01 and 0.02 mol l^{-1},

respectively. (Note, the net peroxide group concentration is twice the initiator concentration.) For low initiator concentrations (e.g. $I_0 = 0.005$ and $0.01\ \text{mol}\,\text{l}^{-1}$) dead end type polymerization occurs at high temperature (100, 110°C) due to a premature peroxide decomposition, resulting in much less than 100% monomer conversion. At $I_0 = 0.02\ \text{mol}\,\text{l}^{-1}$, the dead end polymerization is seen at 110°C. A slight increase in the monomer conversion after the depletion of the peroxides is due to thermal polymerization. When unsymmetrical bifunctional initiators are used, two different slopes are observed at low and intermediate conversions due to the different thermal stabilities of the two peroxide groups[1,2,4]. However, such behaviour is not seen in *Figures 1–3*, indicating that there is no discernible difference in the reactivities of the two peroxide groups in the bifunctional initiator used in this study. [A recent report by Villalobos *et al.*[5] for the same initiator shows a break in the conversion curve at 80–90°C and the monomer conversion at 100°C for $I_0 = 0.01\ \text{mol}\,\text{l}^{-1}$ increases suddenly after 3 h of reaction time (monomer conversion = 68%) at which the concentration of undecomposed peroxide group is <0.25%. It is not clear why the conversion increased to ~95% even after the depletion of the peroxide group. This behaviour was not observed for our experimental data.] *Figures 1–3* also indicate that the gel effect is not quite as strong in the temperature range 90–110°C.

In developing and validating the kinetic model for the bifunctional initiator system, it is necessary to use correct kinetic parameters including f_i. In the kinetic modelling of free radical polymerization with monofunctional initiators, constant f_i is frequently assumed and indeed a satisfactory fit of experimental data is usually obtained. However, f_i may vary during the course of polymerization, in particular as the viscosity of the reaction mixture increases with monomer conversion[12–14]. Kim *et al.*[4] also reported for bulk styrene polymerization with an unsymmetrical bifunctional initiator (4-((tert-butylperoxy) carbonyl)-3-hexyl-6-[7-((tert-butylperoxy) carbonyl)heptyl]cyclohexene) that the overall f_i decreases considerably with an increase in the initiator concentration. With the gel effect correlation parameters and other kinetic parameters fixed, f_i can be used as an adjustable model parameter to fit the experimental monomer conversion data. Assuming that the initial reaction kinetics is similar to the reaction kinetics with monofunctional initiators, f_i can be estimated using the initial polymerization rate ($R_{p,0}$) data, i.e. the following equation is used to estimate f_i:

$$f_i = (R_{p,0}/k_p M_0)^2 k_t/(2k_d I_0') \qquad (19)$$

where I_0' is the concentration of the peroxide groups in the initiator at $t = 0$. If f_i is independent of the initiator concentration, a plot of R_{p0} *versus* $(I_0')^{1/2}$ will give a straight line passing through the origin. *Figure 4* shows such a plot for the experimental data at 90, 100 and 110°C. A slight but clear departure from the straight line passing through the origin is observed at high initiator concentration in each case. If the straight line is assumed for each case, the f_i values obtained by a least square method are 0.467 (90°C), 0.476 (100°C) and 0.487 (110°C). When these f_i values are used, a poor prediction of monomer conversion is obtained for all cases, in particular at high monomer conversion. These f_i values are also inconsistent with the f_i values obtained from

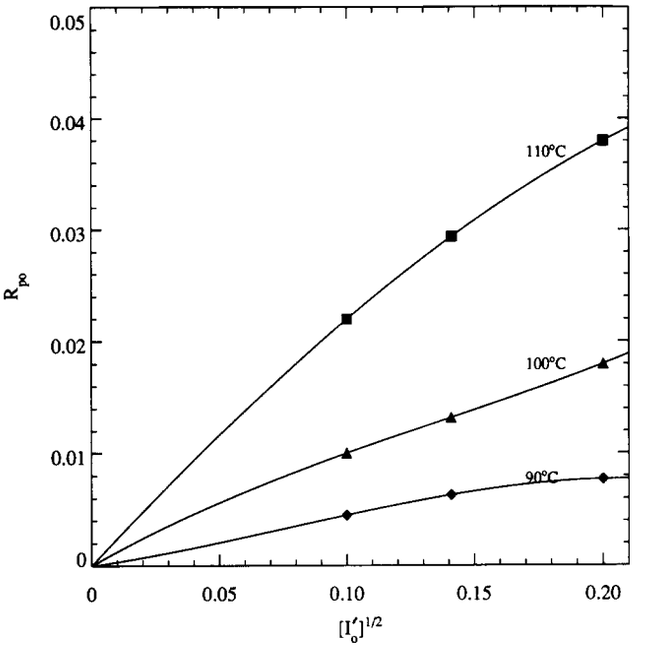

Figure 4 Initial polymerization rate *versus* $[I_0']^{1/2}$

Table 4 Initiator efficiency factor

I_0 (mol l^{-1})	From initial polymerization data [equation (19)]				By optimal search method
	T (°C)				
	90	100	110	Average	
0.005	0.581	0.557	0.567	0.568 ± 0.012	0.586
0.01	0.549	0.488	0.510	0.516 ± 0.031	0.531
0.02	0.423	0.451	0.423	0.432 ± 0.016	0.437

equation (19). Thus, we have also estimated f_i using an optimal parameter search method (Rosenbrock's direct search method) with the experimental monomer conversion data and the kinetic model. Here, the f_i values obtained from the initial reaction rate data [equation (19)] were used as initial guesses for optimization claculations. *Table 4* summarizes the f_i values estimated by using equation (19) and the optimal parameter search method. Note that the f_i values obtained by the two different methods are very close and that the f_i values are relatively insensitive to the temperature variations but strongly dependent on the initiator concentration. It is interesting to observe that the f_i values obtained are lower than those for many monofunctional initiators (e.g. 0.6–0.8). A low overall f_i has also been observed for other multifunctional initiator systems[4,15,16]. In general, the initiator efficiency decreases with an increase in the number of labile groups in the initiator molecule.

The dependence of the efficiency factor on the initiator concentration is shown in *Figure 5* which shows that f_i decreases linearly with an increase in the initiator concentration for the range of initiator concentrations considered in this study. A similar result was also observed for styrene polymerization with an unsymmetrical bifunctional initiator[4]. Heffelfinger and Langsam[17] also reported that the initiator efficiency

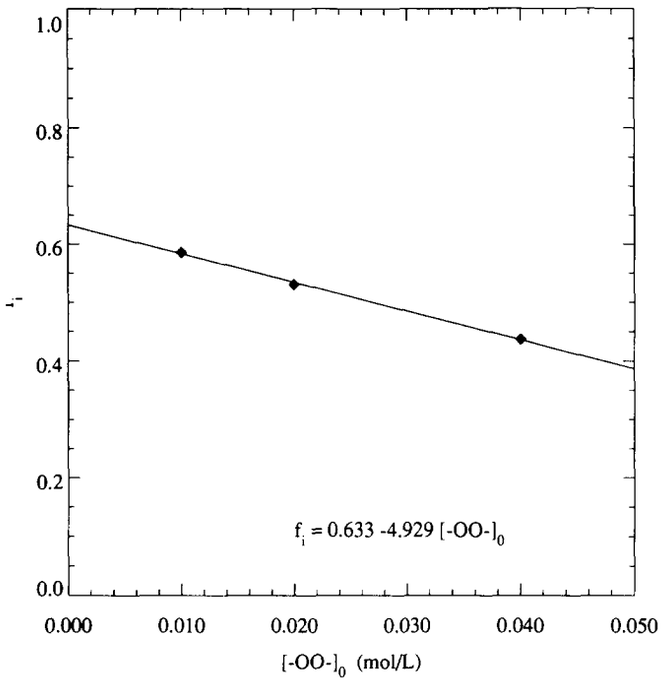

Figure 5 Effect of initial peroxide concentration on f_i

decreases with an increase in the initiator concentration for vinyl chloride–vinyl acetate copolymerization with t-butyl perneodecanoate as an initiator. It should be noted here that the initiator efficiency may vary during the polymerization but we assume that f_i is constant. Thus, the f_i values shown here should be considered to be averaged 'apparent' efficiency values.

Using the f_i values obtained by the optimal parameter search method, we solved the kinetic model which consists of the rate equations and the molecular weight moment equations. The solid lines in *Figures 1–3* are the monomer conversion profiles predicted by the model. Over the entire range of reaction temperature and initiator concentration, the agreement between the model predictions and the experimental data is very satisfactory.

The polymer molecular weight averages (M_n and M_w) are shown in *Figures 6–8*. For all the polymer samples analysed, no bimodality in the molecular weight distribution curves was observed. These figures indicate that the number average molecular weights predicted by the model are in good agreement with the experimental data, and as expected, higher molecular weights are obtained at lower initiator concentrations and reaction

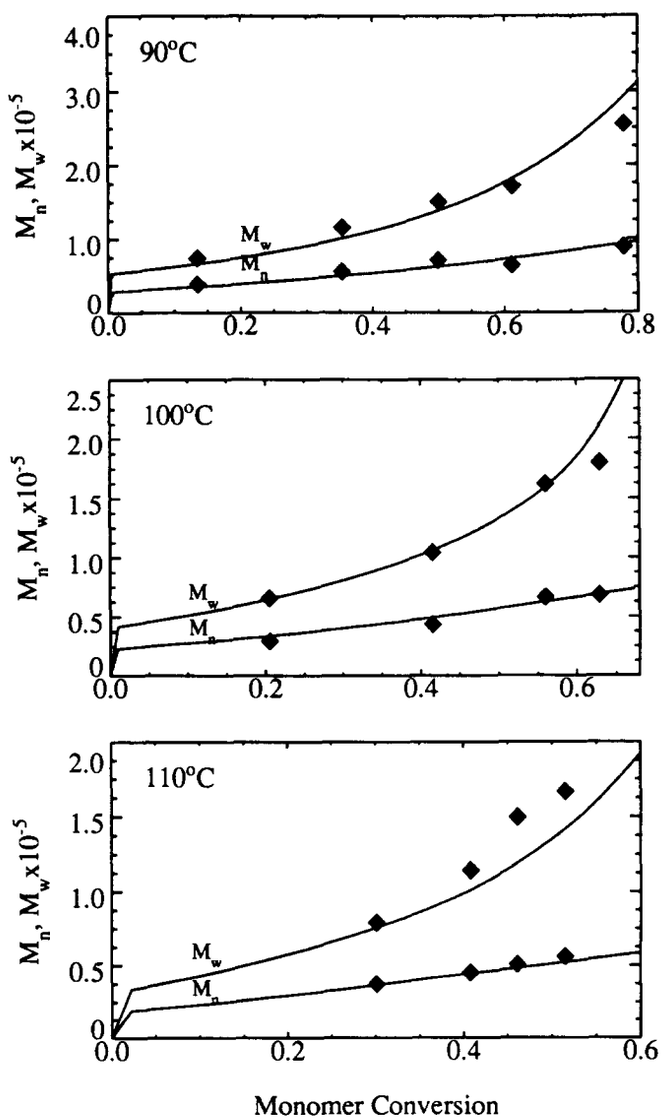

Figure 6 Effect of polymerization temperature on M_n and M_w ($I_0 = 0.005$ mol l^{-1}; ——, model prediction)

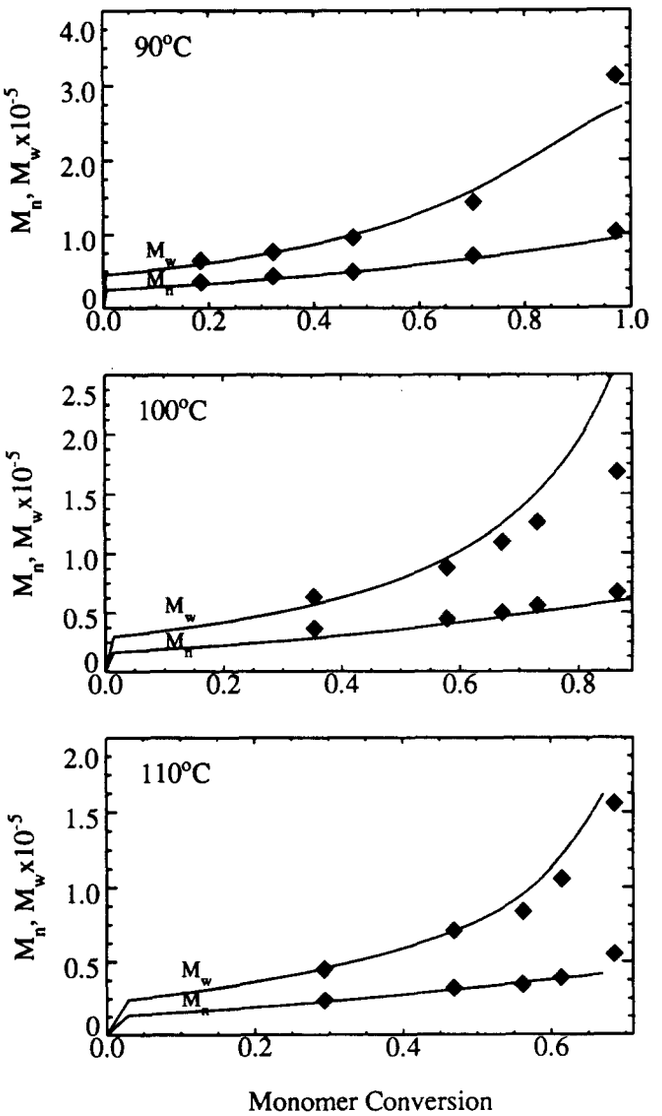

Figure 7 Effect of polymerization temperature on M_n and M_w ($I_0 = 0.01$ mol l^{-1}; ——, model prediction)

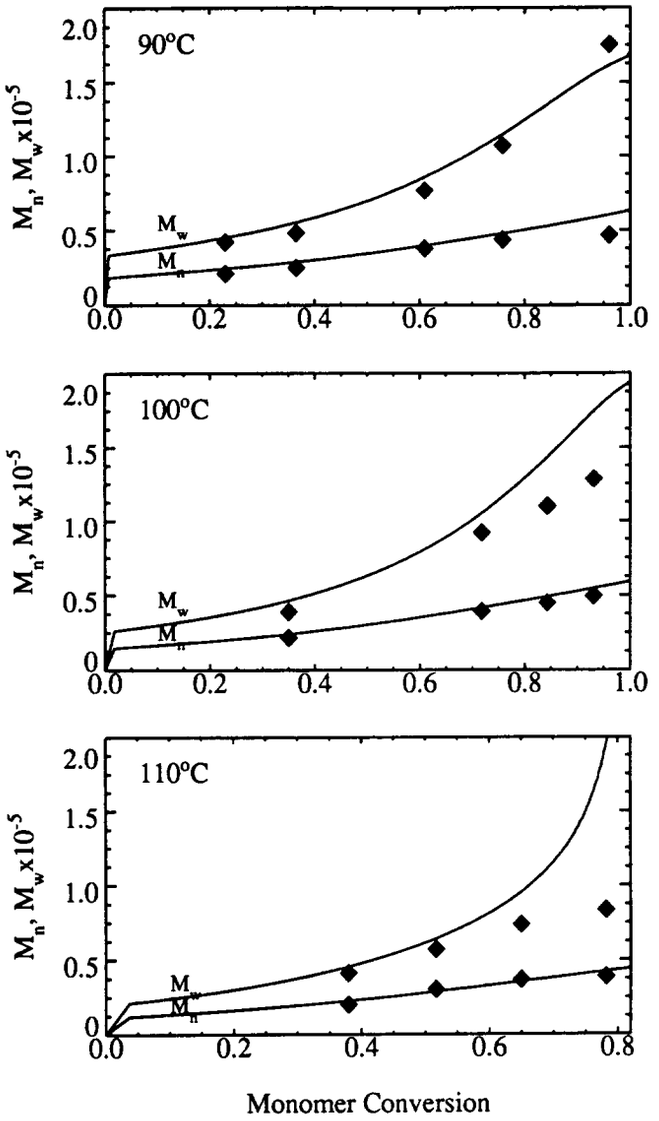

Figure 8 Effect of polymerization temperature on M_n and M_w ($I_0 = 0.02$ mol l^{-1}; ——, model prediction)

temperatures. Our experimental data also show that the polydispersity values (M_w/M_n) lie in the range 2.0–3.0. The polydispersity increases as the monomer conversion increases. A few factors which may cause the molecular weight distribution broadening are gel effect, primary radical termination and the multiple reactions (e.g. initiation, propagation and combination termination) that some polymers containing undecomposed peroxides may undergo. Initially, it was assumed that only the termination rate constant is affected by the gel effect and very satisfactory predictions of monomer conversion were obtained. However, it was observed that the predicted polymer molecular weight values were almost always lower than the experimental data, in particular at high monomer conversion. Such discrepancies may be due to some simplifying assumptions employed in the model (e.g. equal thermal stability of the peroxides, no primary radical termination and constant initiator efficiency) or any unknown mechanisms which are unmodelled. In practice, it is very difficult to point out what mechanism has caused the discrepancy and to what extent. Without quantitative understanding of the underlying microscopic molecular phenomena there are not many alternatives but to introduce adjustable parameters to fit the data. Or course, if possible, it is desirable to minimize the number of such adjustable parameters. Since the polymer molecular weight is quite sensitive to the value of the chain transfer rate constant (k_{fm}) which has negligible influence on the monomer conversion, it was decided to use k_{fm} as a model tuning parameter. Thus, the k_{fm} value was multiplied by the gel effect correlation factor (g_t) used in the termination rate constant. We found that this empirical approach gave an improved prediction of polymer molecular weight averages as shown in *Figures 6–8*. The use of this modified k_{fm} does not affect the monomer conversion or the polymerization rate. It must be pointed out that little experimental evidence has been reported on the effect of diffusion controlled chain transfer reactions. There is also a possibility that the peroxides may exhibit different thermal stabilities before and after the decomposition of the first peroxide, affecting the reaction kinetics and polymer molecular weight properties. In our model simulations, the decomposition rate constant reported by the initiator manufacturer was used and the reactivity of the peroxides in the initiator was assumed to be equal.

The concentration profiles of live polymers (P, Q) are shown in *Figure 9*. The concentrations of primary radicals and diradical species (S) are so low that they are not shown. The vertical broken lines indicate the points where the peroxides are completely decomposed. A quick observation of *Figure 9* indicates that the concentrations of P and Q are strongly affected by both reaction temperature and the initiator concentration. It is interesting to observe that at 90°C with $I_0 = 0.02$ mol l^{-1}, the concentration of Q radicals (polymer radical with an undecomposed peroxide) reaches a maximum at 85% monomer conversion and then decreases. At low initiator concentration (e.g. $I_0 = 0.005$ or 0.01 mol l^{-1}) and high

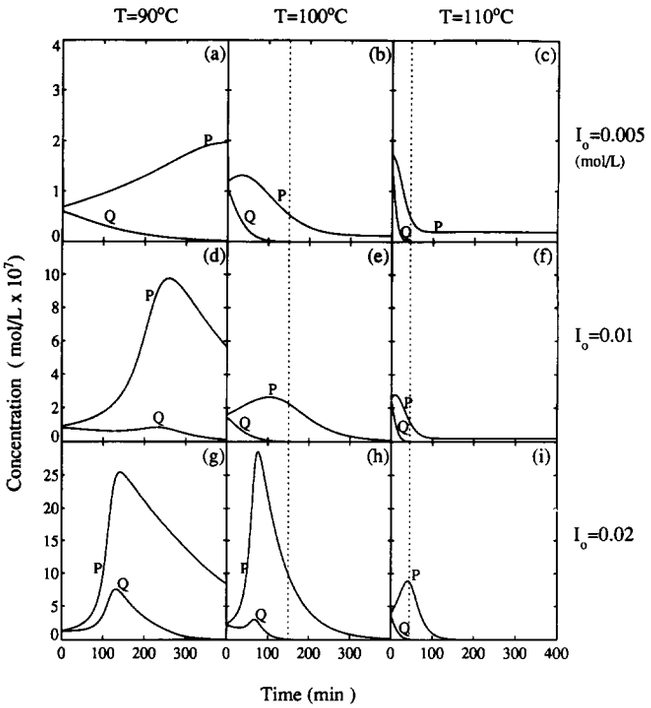

Figure 9 Effect of initiator concentration and reaction temperature on the concentration profiles of live polymers. Vertical lines indicate the points where the peroxides are completely decomposed

temperature (e.g. 110°C), the concentration of Q radicals decreases monotonically from the beginning of polymerization.

The fate of undecomposed peroxide in the primary initiator (I) and inactive polymers (Z and T) during the polymerization is shown in *Figure 10*. Here, O_j is the peroxide concentration in the species j. Since the reactivity of the peroxide is assumed to be independent of the type of molecules to which it is attached, the O_j profiles are affected only by reaction temperature. Note that as the reaction proceeds to above a certain monomer conversion, more peroxides are present in the polymeric species (e.g. Z) than in the primary initiator. However, the concentration of such 'polymeric peroxide' is quite low that its use for sequential block copolymerization will be ineffective. *Figure 10* indicates that the concentration of polymeric initiators can be increased by employing low reaction temperature that slows down the decomposition of the peroxides. When unsymmetrical bifunctional initiators containing two peroxides of quite different thermal stabilities are used it is easier to obtain a large amount of polymeric initiators containing undecomposed and more stable peroxides. It is also seen in *Figure 10* that at 100 and 110°C, the concentration of T species having two undecomposed peroxides is negligibly small.

It is necessary to refer to the need for a detailed kinetic model as presented in this paper for free radical polymerization with bifunctional initiators. Let us again assume that the decomposition rate of the peroxide is

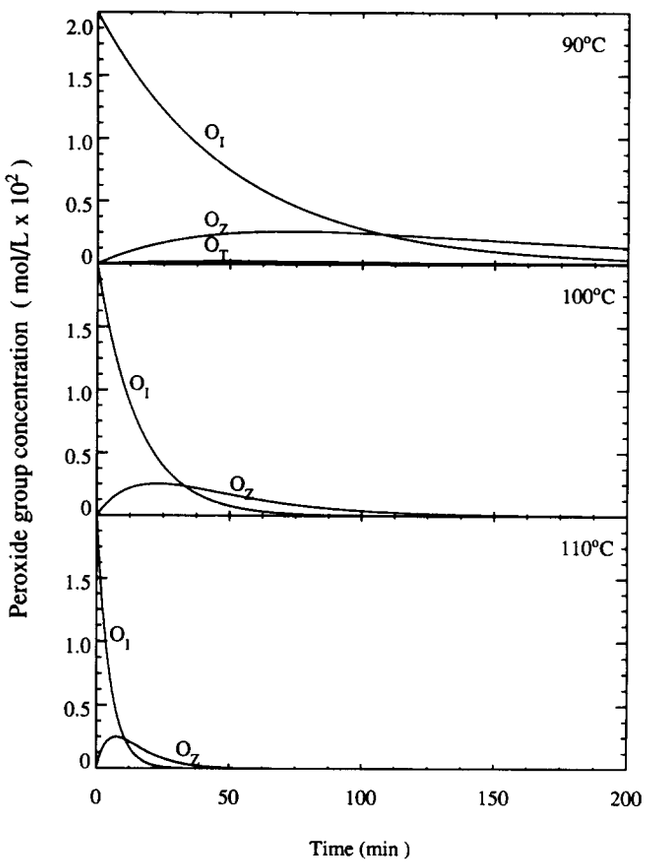

Figure 10 Variations of peroxide group concentration in the primary initiator and polymeric species during polymerizations ($I_0 = 0.01$ mol l^{-1})

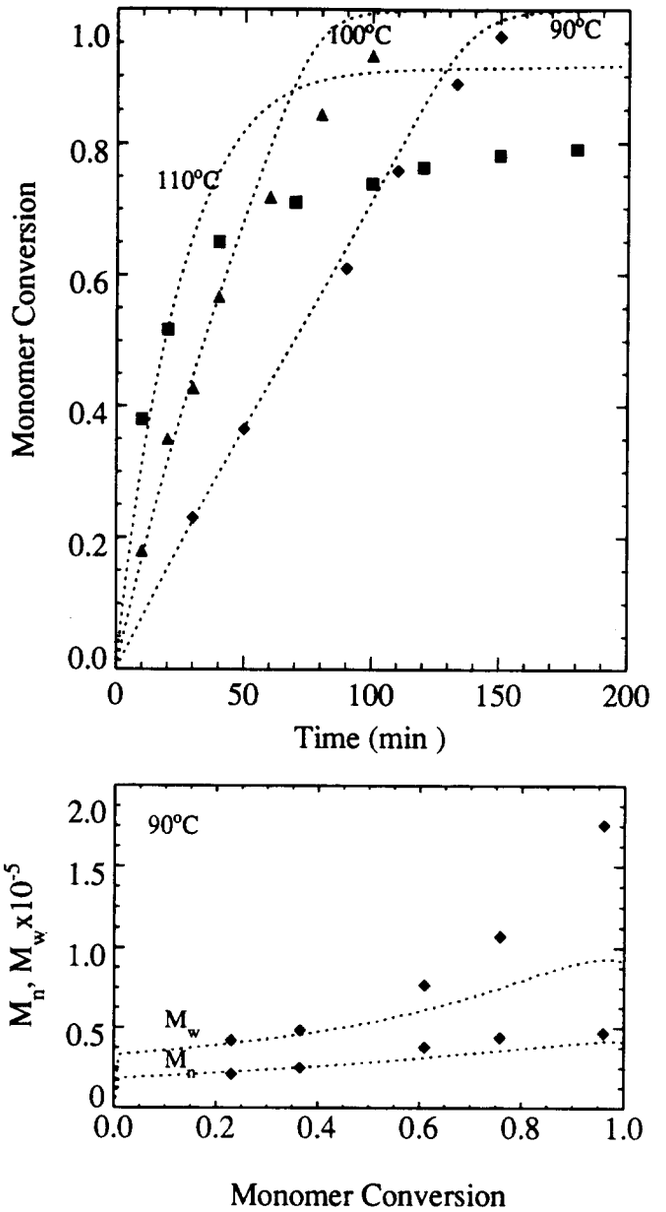

Figure 11 Test of a kinetic model for monofunctional initiators ($I_0 = 0.04$ mol l^{-1})

unaffected by the chain length of the polymer to which the peroxide group is attached. Then, one can postulate, as an approximation, that using the bifunctional initiator is just to double the concentration of peroxide groups and that the kinetic model for monofunctional initiators can be used. Using the kinetic model for bulk styrene polymerization with monofunctional initiators, model simulations were conducted. Here, the thermal initiation, volume change and gel effect were included and the same kinetic parameters used in the bifunctional initiator model were used. *Figure 11* shows the resulting model simulations compared with experimental data. It is seen that the monofunctional model (broken lines) yields a poor prediction of monomer conversion and polymer molecular weight. In particular, the predicted molecular weight values at 90°C are much lower than those predicted by the bifunctional initiator model. (The monomer conversion at 90°C predicted by the simple model is reasonably good.) This implies that the bifunctional initiator, albeit symmetrical, can produce

polymers of higher molecular weight than the monofunctional initiators having the same thermal decomposition characteristics. This is because the presence of 'polymeric initiators' (e.g. Q, Z and T species) extend the polymer chain length through peroxide decomposition and combination termination reactions. Thus, this test clearly indicates that for the quantitative description of the polymerization kinetics with bifunctional initiators, a detailed molecular species model as presented in this paper will be very useful.

CONCLUSIONS

A molecular species model has been developed and solved for the quantitative analysis of styrene polymerization with symmetrical bifunctional initiators. The experimental and model simulation results show that the kinetic model is adequate in predicting the progress of reaction and the resulting polymer molecular weight properties. At high monomer conversion the M_w increases rapidly and, as a result, a broad molecular weight distribution (M_w/M_n = 2.0–3.0) is obtained. In our modelling work the modified k_{fm} ($= k_{fm,0}g_t$) was used and a satisfactory fit with the experimental results was obtained. It has also been shown that the kinetic model can be used to estimate the concentration of various polymeric species. The maximum concentration of 'polymeric initiators' (polymers containing undecomposed peroxides) is obtained when high initiator concentration is employed at low reaction temperatures. In principle, it will be possible to produce block copolymers by sequential monomer addition technique with such polymeric initiators. For the range of initiator concentrations employed in this work (0.005–0.02 mol l^{-1}), the apparent f_i was found to decrease linearly with initiator concentration. However, the initiator efficiency was little affected by polymerization temperature.

ACKNOWLEDGEMENTS

Acknowledgement is made to the Donors of the Petroleum Research Funds, administered by the American Chemical Society, for support of this research (20223-AC7). Partial support was also provided by the National Science Foundation (CBT-85-52428).

REFERENCES

1 Choi, K. Y. and Lei, G. D. *AIChE J.* 1987, **20**, 2067
2 Kim, K. J. and Choi, K. Y. *Chem. Eng. Sci.* 1988, **44**, 197
3 Choi, K. Y., Liang, W. R. and Lei, G. D. *J. Appl. Polym. Sci.* 1988, **35**, 1547
4 Kim, K. J., Liang, W. and Choi, K. Y. *Ind. Eng. Chem. Res.* 1989, **28**, 131
5 Villalobos, M. A., Hamielec, A. E. and Wood, P. E. *J. Appl. Polym. Sci.* 1991, **42**, 629
6 Friis, N. and Hamielec, A. E. *Am. Chem. Soc. Symp. Ser.* 1976, **24**, 82
7 Ray, W. H. *J. Macromol. Sci. Rev. Macromol. Chem.* 1972, **C8**(1), 1
8 Technical Bulletin, Pennwalt-Lucidol Company, Buffalo, 1986
9 Hui, A. W. and Hamielec, A. E. *J. Appl. Polym. Sci.* 1972, **16**, 749
10 Brandrup, J. and Immergut, E. H. 'Polymer Handbook', 3rd Edn, Wiley, New York, 1990
11 Arai, K., Yamaguchi, H., Saito, S., Sarschina, E. and Yamamoto, T. *J. Chem. Eng. Jpn* 1986, **19**, 413
12 Bevington, J. C. *Trans. Faraday Soc.* 1955, **51**, 1392
13 Moad, G., Rizardo, E., Solomon, D. H., Johns, S. R. and Willing. R. I. *Makromol. Chem. Rapid Commun.* 1984, **5**, 793
14 Russel, G. T., Napper, D. H. and Gilbert, R. G. *Macromolecules* 1988, **21**, 2141
15 Vuillemont, J., Barbier, B., Riess, G. and Banderet, A. *J. Polym. Sci. A* 1965, **3**, 1969
16 Ivanchev, S. S. and Zherebin, Y. I. *Polym. Sci. USSR* 1974, **16**, 956
17 Heffelfinger, M. T. and Langsam, M. *J. Appl. Polym. Sci.* 1985, **30**, 3377

APPENDIX

Molecular weight moment equations

Polymeric species P_n:

$$\frac{1}{V}\frac{d(\lambda_{P,0}V)}{dt}\left[=\frac{1}{V}\frac{d(PV)}{dt}\right]=2k_m M^3+k_i RM+k_d Z+k_{fm}M(Q+4S)-k_t P(P+Q) \quad (A1)$$

$$\frac{1}{V}\frac{d(\lambda_{P,1}V)}{dt}=2k_m M^3+k_i RM+k_d\lambda_{Z,1}+k_{fm}M(P-\lambda_{P,1}+Q+2S+2\lambda_{S,1})+k_p MP+k_t[2P\lambda_{S,1}-(P+Q)\lambda_{P,1}] \quad (A2)$$

$$\frac{1}{V}\frac{d(\lambda_{P,2}V)}{dt}=2k_m M^3+k_i RM+k_d\lambda_{Z,2}+k_{fm}M(P-\lambda_{P,2}+Q+2S+2\lambda_{S,2})+k_p M(2\lambda_{P,1}+P)+k_t[4\lambda_{S,1}\lambda_{P,1}+2\lambda_{S,2}P-(P+Q)\lambda_{P,2}] \quad (A3)$$

Polymeric species Q_n:

$$\frac{1}{V}\frac{d(\lambda_{Q,0}V)}{dt}\left[=\frac{1}{V}\frac{d(QV)}{dt}\right]=k_i R_A M+k_d(2T-Q)-k_{fm}MQ-k_t Q(P+Q) \quad (A4)$$

$$\frac{1}{V}\frac{d(\lambda_{Q,1}V)}{dt}=k_i R_A M+k_d(2\lambda_{T,1}-\lambda_{Q,1})-k_{fm}M\lambda_{Q,1}+k_p MQ+k_t[2\lambda_{S,1}Q-(P+Q)\lambda_{Q,1}] \quad (A5)$$

$$\frac{1}{V}\frac{d(\lambda_{Q,2}V)}{dt}=k_i R_A M+k_d(2\lambda_{T,2}-\lambda_{Q,2})-k_{fm}M\lambda_{Q,2}+k_p M(2\lambda_{Q,1}+Q)+k_t[4\lambda_{S,1}\lambda_{Q,1}+2\lambda_{S,2}Q-(P+Q)\lambda_{Q,2}] \quad (A6)$$

Polymeric species S_n:

$$\frac{1}{V}\frac{d(\lambda_{S,0}V)}{dt}\left[=\frac{1}{V}\frac{d(SV)}{dt}\right]=2k_i R'M+k_d Q-2k_{fm}MS-2k_t[S(P+Q)+S^2] \quad (A7)$$

$$\frac{1}{V}\frac{d(\lambda_{S,1}V)}{dt}=2k_i R'M+k_d\lambda_{Q,1}-2k_{fm}M\lambda_{S,1}+2k_p MS-2k_t(P+Q)\lambda_{S,1} \quad (A8)$$

$$\frac{1}{V}\frac{d(\lambda_{S,2}V)}{dt}=2k_i R'M+k_d\lambda_{Q,2}-2k_{fm}M\lambda_{S,2}+2k_p M(2\lambda_{S,1}+S)+k_t[4\lambda_{S,1}^2-2(P+Q)\lambda_{S,2}] \quad (A9)$$

Polymeric species T_n:

$$\frac{1}{V}\frac{d(\lambda_{T,0}V)}{dt}\left[=\frac{1}{V}\frac{d(TV)}{dt}\right]=-2k_dT+\frac{k_t}{2}Q^2 \quad (A10)$$

$$\frac{1}{V}\frac{d(\lambda_{T,1}V)}{dt}=-2k_d\lambda_{T,1}+k_t\lambda_{Q,1}Q \quad (A11)$$

$$\frac{1}{V}\frac{d(\lambda_{T,2}V)}{dt}=-2k_d\lambda_{T,2}+k_t(\lambda_{Q,2}Q+\lambda_{Q,1}^2) \quad (A12)$$

Polymeric species Z_n:

$$\frac{1}{V}\frac{d(\lambda_{Z,0}V)}{dt}\left[=\frac{1}{V}\frac{d(ZV)}{dt}\right]=-k_dZ+k_{fm}MQ+k_tPQ \quad (A13)$$

$$\frac{1}{V}\frac{d(\lambda_{Z,1}V)}{dt}=-k_d\lambda_{Z,1}+k_{fm}M\lambda_{Q,1}+k_t(\lambda_{P,1}Q+\lambda_{Q,1}P) \quad (A14)$$

$$\frac{1}{V}\frac{d(\lambda_{Z,2}V)}{dt}=-k_d\lambda_{Z,2}+k_{fm}M\lambda_{Q,2}+k_t(\lambda_{P,2}Q+2\lambda_{P,1}\lambda_{Q,1}+\lambda_{Q,2}P) \quad (A15)$$

Dead polymers:

$$\frac{1}{V}\frac{d(\lambda_0^dV)}{dt}=k_{fm}M(P-P_1)+\frac{k_t}{2}P^2 \quad (A16)$$

$$\frac{1}{V}\frac{d(\lambda_1^dV)}{dt}=k_{fm}M(\lambda_{P,1}-P_1)+k_tP\lambda_{P,1} \quad (A17)$$

$$\frac{1}{V}\frac{d(\lambda_2^dV)}{dt}=k_{fm}M(\lambda_{P,2}-P_1)+k_t(P\lambda_{P,2}+\lambda_{P,1}^2) \quad (A18)$$

Primary radical concentrations

$$R_A=\frac{2f_ik_dI}{k_d+k_iM} \quad (A19)$$

$$R'=\frac{f_ik_dR_A}{2k_iM} \quad (A20)$$

$$R=\frac{f_i}{k_iM}[2k_dI+k_d(Q+2T+Z)] \quad (A21)$$

Zeroth moments of live polymers (calculated by solving the following equations)

$$k_tP^2+k_tQP-2k_mM^3-k_iRM-k_dZ-k_{fm}M(Q+4S)=0 \quad (A22)$$

$$k_tQ^2+(k_tP+k_d+k_{fm}M)Q-2k_dT-k_iR_AM=0 \quad (A23)$$

$$k_tS^2+[k_t(P+Q)+k_{fm}M]S-\frac{1}{2}k_dQ-k_iR'M=0 \quad (A24)$$

First moments of live polymers

$$\lambda_{P,1}=\frac{2(k_{fm}M+k_tP)\lambda_{S,1}+A_1}{k_{fm}M+k_t(P+Q)} \quad (A25)$$

$$\lambda_{Q,1}=\frac{2k_tQ\lambda_{S,1}+B_1}{k_d+k_{fm}M+k_t(P+Q)} \quad (A26)$$

$$\lambda_{S,1}=\frac{C_{1A}}{2C_{1B}} \quad (A27)$$

where

$$A_1=2k_mM^3+k_iRM+k_d\lambda_{Z,1}+k_pMP+k_{fm}M(P+Q+2S) \quad (A28)$$

$$B_1=k_iR_AM+2k_d\lambda_{T,1}+k_pMQ \quad (A29)$$

$$C_{1A}=2k_iR'M+\frac{k_dB_1}{k_d+k_{fm}M+k_t(P+Q)}+2k_pMS \quad (A30)$$

$$C_{1B}=k_{fm}M+k_t(P+Q)-\frac{k_dk_tQ}{k_d+k_{fm}M+k_t(P+Q)} \quad (A31)$$

Second moments of live polymers

$$\lambda_{P,2}=\frac{2(k_{fm}M+k_tP)\lambda_{S,2}+A_2}{k_{fm}M+k_t(P+Q)} \quad (A32)$$

$$\lambda_{Q,2}=\frac{2k_tQ\lambda_{S,2}+B_2}{k_d+k_{fm}M+k_t(P+Q)} \quad (A33)$$

$$\lambda_{T,2}=\frac{C_{2A}}{2C_{2B}} \quad (A34)$$

where

$$A_2=2k_mM^3+k_iRM+k_d\lambda_{Z,2}+k_pM(2\lambda_{P,1}+P)+k_{fm}M(P+Q+2S)+4k_t\lambda_{P,1}\lambda_{S,1} \quad (A35)$$

$$B_2=k_iR_AM+2k_d\lambda_{T,2}+k_pM(2\lambda_{Q,1}+Q)+4k_t\lambda_{Q,1}\lambda_{S,1} \quad (A36)$$

$$C_{2A}=2k_iR'M+\frac{k_dB_2}{k_d+k_{fm}M+k_t(P+Q)}+2k_pM(2\lambda_{S,1}+S)+4k_t\lambda_{S,1}^2 \quad (A37)$$

$$C_{2B}=k_{fm}M+k_t(P+Q)-\frac{k_dk_tQ}{k_d+k_{fm}M+k_t(P+Q)} \quad (A38)$$